Static and dry friction due to multiscale surface roughness

J. B. Sokoloff
Physics Department and Center for Interdisciplinary Research in Complex Systems, Northeastern University, Boston, Massachusetts 02115, USA

(Received 13 May 2008; revised manuscript received 20 June 2008; published 10 September 2008)

It is shown on the basis of scaling arguments that a disordered interface between two elastic solids will quite generally exhibit static and dry friction (i.e., kinetic friction which does not vanish as the sliding velocity approaches zero) because of Tomlinson-model instabilities that occur for small-length-scale asperities. This provides a possible explanation for why static and dry friction are virtually always observed, and superlubricity almost never occurs.

DOI: 10.1103/PhysRevE.78.036111 PACS number(s): 81.40.Pq, 68.35.Af, 46.55.+d

I. INTRODUCTION

A few years ago, Muser and Robbins [1] proposed that static friction between clean crystalline solid surfaces, whose crystal axes were rotated by an arbitrary angle with respect to each other so that the surfaces are incommensurate, would be zero. This is commonly known as superlubricity [2]. The apparent lack of friction for crystalline surfaces rotated by an arbitrary angle with respect to each other (which is the most common configuration) appears to go against common experience that almost all solid surfaces exhibit static friction. In order to explain the fact that superlubricity is rarely observed, they then proposed that the likely source of static friction for such surfaces is the existence of mobile dirt molecules, always present at any interface. The mobile molecules seek out local energy minima at the interface, which results in the surfaces being pinned with respect to each other; i.e., there is static friction. In fact, there can also be superlubricity for smooth disordered surfaces. In Refs. [3,4] it was argued that a flat disordered interface between two macroscopic-size surfaces which do not interact chemically will exhibit effectively no static friction for interface interaction per unit interface area small compared to the shear elastic constant and high friction for interface interaction above this value. This frictionless regime is known as the weak-pinning regime and the large friction regime is known as the strong-pinning regime. In Ref. [3], I argued that the existence of micron-length-scale asperities at an interface can result in both slow speed kinetic friction (often referred to as dry friction) and static friction, resulting from the fact that these asperities can occur in multistable equilibrium configurations, which result in dry friction as a consequence of the Tomlinson model [5] and static friction as well. The requirement for asperities being multistable is that the force on an asperity on one surface due to its interaction with a second surface dominate over the elastic forces resulting from its distortion, as a consequence of its interaction with the second surface. Since the interaction of an asperity with the second surface varies on atomic length scales, the distance over which the asperity distorts is negligibly small compared with its size (about a micron). Since micron length scales are still large compared with atomic spacings, however, the resulting static and dry friction is still likely to be quite small, indicating that the Muser-Robbins picture is still basically correct.

The basic idea of Ref. [6] and the work presented here is as follows: Any rough surface has asperities on multiple length scales, which means, for example, that if there are asperities on the micron scale, the interface between two of these asperities in contact will have a bunch of smaller than micron scale asperities in contact. At the interface between a pair of these smaller-scale asperities there are still smaller-scale asperities in contact. This continues until we reach atomic scales. The smallest length scale (the one just before one reaches atomic dimensions) is denoted by L_0. These are the asperities that are actually in contact with the second surface, and hence they must support all of the load. As we attempt to slide the surfaces relative to each other, asperities on all length scales are distorted. If the asperity's interaction with the second surface is large enough compared with the asperity's elastic energy, an asperity at a given length scale can exhibit Tomlinson-model instabilities [5]. (Note that the force exerted by the second surface on all asperities at all length scales above L_0 is transmitted through smaller-length-scale asperities at the interface between this asperity and the second surface.) These instabilities will result in nonzero dissipation even in the limit of vanishing sliding velocity, which will give rise to dry friction (i.e., nonzero kinetic friction in the slow-sliding-speed limit), and one can argue that if there is dry friction, there will also be static friction [5]. The simulation work presented in Ref. [7] supports this picture for the case in which the potential acting across the interface is exponential, in the sense that it finds static friction for self-affine surfaces, whereas when a hard-wall potential is used, static friction does not occur (i.e., there is "superlubricity"). The model interface potential used in Ref. [6] gives rise to a force component along the surface, which makes it act effectively more like the exponential than the hard-wall potential model of Ref. [7]. In Ref. [6], scaling arguments were used to establish criteria for the occurrence of these instabilities on all length scales. The purpose of that publication was to suggest a possible mechanism for why stiff and hard carbon films, treated with hydrogen to saturate dangling bonds at the surface, should be excellent lubricants. Up to now, most of the experimental studies of these materials have focused on the question of how the hydrogen affects the lubricating properties of these films, by saturating the dangling bonds at the interface [8]. The question raised in Ref. [6] and the present study is that once the bonds are saturated, what possible mechanism can there be for stiff films being good lubricants? Plasticity (which was not discussed in Ref. [6], but is discussed here) will likely play an important role for small-length-scale asperities as well. It will be argued that plastic deformation under the high degree of stress acting on the small-length-scale asperities will enhance the tendency for multistability to occur for these asperities, resulting in an increased tendency for the occurrence of static and dry friction. Recent work on contact mechanics [9,10] makes it possible to provide a more complete treatment of the scaling theory of Ref. [6], allowing a more numerical study of the conditions under which static friction can arise as a consequence of multiscale roughness, without the need to postulate that static and dry friction can only occur when there are mobile ion dirt particles present at the interface [1], at least for surfaces that can be modeled as self-affine over a few length scales. Combining the scaling theory of Ref. [6] with the analytic contact mechanics theory of Ref. [10] allows us to relate the occurrence of static and dry friction (i.e., kinetic friction in the slow-sliding-speed limit) to the contact area at various length scales. It also allows us to determine the conditions under plastic deformation is expected to be important, and a discussion is given of how plastic deformation affects the occurrence of static and dry friction. By combining the results of Refs. [6,10], it was possible to make more precise statements than was possible using the methods of Ref. [6] alone concerning the conditions under which surfaces coated with materials with high-shear elastic constants will lead to low friction, by expressing the criterion for this to occur in terms of parameters describing the nature of the roughness of the surface, in addition to the elastic constants.

The next section summarizes the results of Ref. [6] and makes some improvements and corrections. In Sec. III, the scaling theory of Ref. [6] is expressed in the language of Persson's theory of contact mechanics [10], and the results of this theory are used to obtain information on the conditions under which large static and dry friction are likely to occur.

II. EFFECTS OF ROUGHNESS (ASPERITIES ON SEVERAL LENGTH SCALES)

As in Ref. [6], we consider two surfaces in contact which are disordered so that those atoms which are in contact are randomly distributed over the interface. In order to simplify the discussion, we will consider as our model for the interface a rough elastic surface in contact with a perfectly atomically flat rigid surface. This has been argued in the past to be equivalent to the more correct model of two rough elastic surfaces in contact, for the contact mechanics problem, in which there are only forces normal to the surface [9–11]. While it is not a rigorously correct representation of the problem when there are frictional (i.e., shear) stresses present as well, it should give correct orders of magnitude for the scaling treatment considered on Ref. [6] and here. Let us also assume that the atoms in contact at the interface interact only with hard-core interactions. This could occur either because the surface atoms are chemically inert and there is negligible adhesion or because the surfaces are being pushed together with a sufficient load so that the hard core interactions dominate. Let σ denote the load or normal force per unit interface

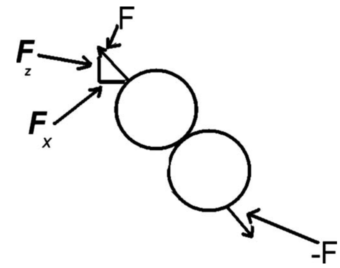

FIG. 1. This figure illustrates how the hard-core interaction between a pair of atoms, one belonging to each of the surfaces in contact, can both support the load and give rise to static friction between the surfaces. Since the force F between the pair of atoms can have both a component normal to the interface, F_z, which contributes to the normal force supporting the load, and a component along the interface, F_x, the mean value of F_x must be proportional to the mean value of F_z.

area; a, the mean atomic spacing; and c, the fraction of the surface atoms of one surface that are in contact with the second surface. Then, each of the atoms in contact must contribute on average to the normal force a force, of order $\sigma a^2/c$. Since the force due to the hard-core interaction between a pair of atoms acts along the line joining the atoms, for most relative positions of the atoms, it has a component along the interface, as illustrated in Fig. 1.

The surfaces are assumed to be rough on n_m length scales as illustrated schematically in Fig. 2. The n_m length scale denotes the overall length and width of the interface, and $n=0$ denotes the smallest length scale. Asperities at the $n=0$ length scale contain atoms that are in contact with the flat substrate, which represents the second surface. Consider the zeroth-, the lowest-order (i.e., the smallest) asperity first. Let it have a height of order L_0' and a width of order L_0. To find its distortion resulting from the sum of the substrate potential energies of all of the atoms of the asperity which are in contact with the substrate, we must minimize the sum of its elastic and substrate potential energies. The substrate potential energy is given by $V_0(c_a^{1/2}L_0/a)f_0(\Delta x_0/a)$, where V_0 is the amplitude of the interaction of a single atom with the substrate, resulting primarily from hard-core repulsions between the atoms, c_a is the mean fraction of atoms at the interface which are in contact with the substrate, Δx_0 is the amount that the surface in contact with the substrate slides

Asperity Hierarchy

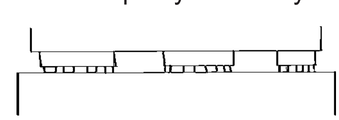

FIG. 2. This is a schematic illustration of the asperity hierarchy on the top surface sliding on a flat substrate (i.e., the bottom block). (Real asperities have arbitrary shapes, as opposed to the square shapes shown in this schematic representation.) Each asperity of a given order has a number of (smaller) asperities of one order lower on its surface. In turn, each of these lower-order asperities has a number of (smaller) asperities of one order lower. This continues until we reach the zeroth-order asperity, whose surface consists of atoms, although only three orders of asperities are illustrated here.

under the influence of the substrate potential as the asperity distorts while all higher-level asperities remain in an arbitrary rigid configuration, and $f_0(\Delta x_0/a)$ is a function of order unity which gives the variation of the substrate potential with Δx_0 for fixed, undistorted asperities of higher order (i.e., larger size in the present context). (Clearly, each of the zeroth-order asperities has a different function; f_0 denotes a generic function describing the interface potential energy for a typical zeroth-order asperity.) Each function clearly must possess multiple minima. We are assuming here that the surface of the asperity in contact with the substrate is in the weak-pinning limit [4]. The factor $(c_a^{1/2}L_0/a)$, which is of the order of the square root of the number of atoms in this surface, expresses this fact. If the surface of the asperity in contact with the substrate is in the strong-pinning limit instead, this factor will be replaced by $c_a(L_0/a)^2$, the number of atoms at the interface. (The factors of $c_a^{1/2}$ and c_a, respectively, in these expressions were inadvertently not included in Ref. [6].) Treating this asperity as an elastic three-dimensional solid in contact with the substrate we find from the discussion in Ref. [4] that the interface between the substrate and this asperity is in the weak-pinning limit if $\sigma_0 < c_a^{1/2}K$, where σ_0 is the mean load per unit interface area supported by this asperity. Assume that a fraction c_0 of the zeroth-order asperities have atoms belonging to them in contact with the substrate. Let c_1 represent the fraction of next-order (first-order) asperities whose zeroth-order asperities are in contact with the substrate, c_2, the fraction of second-order asperities whose first-order asperities have their zeroth-order asperities in contact with the substrate, etc., up to (n_m)th order. Then $\sigma_0=\sigma/(c_0c_1c_2\cdots c_{n_m-1})$, where σ is the load per unit apparent area of the surface of the whole solid. Then, we conclude that the criterion for the atoms at the interface between the zeroth-order asperity and the substrate to be in the weak-pinning regime is that $\sigma<(c_a^{1/2}c_0c_1c_2\cdots c_{n_m-1})K$. We see from this inequality that the more fractal the surface is, the more difficult it is for the zeroth-order asperity to be in the weak-pinning regime. The cost in elastic energy due to the shear distortion of the asperity can be determined by the following scaling argument: The elastic energy density for shear distortion of the asperity is proportional to $(\partial u_x/\partial z)^2$, where u_x represents the local displacement due to the distortion, the x direction is along the interface, and the z direction is normal to it. The u_x must scale with Δx_0, and the dependence of u_x on z has a length scale L_0'. Thus the elastic strain energy of the asperity is of the order of $(1/2)L_0^2L_0'K(\Delta x_0/L_0')^2$, where K is the shear elastic constant and $(\Delta x_0/L_0')$ is the average shear strain and L_0 is the mean width of the asperity. Using a perhaps more correct nonrectangular shape for the asperities is shown in Appendix A to only produce a correction of order unity. Minimizing the sum of these expressions for elastic and substrate potential energy, we obtain

$$\Delta x_0/a \approx (V_0/Ka^3)c_a^{1/2}(L_0'/L_0)f_0'(\Delta x_0/a) \quad (1)$$

since f_0', the derivative of f_0 with respect to its argument, is of order 1, from the definition of f_0. Let us follow a line of reasoning like that of Ref. [5], a modified version of which is given in Ref. [6]. For $(V_0/Ka^3)c_a^{1/2}(L_0'/L_0)$ below a certain value of order 1, for small V_0/Ka^3, Eq. (1) can have only one solution for Δx_0. The reason for this is illustrated in Fig. 3. Under such circumstances the average kinetic friction, in the limit as the sliding velocity approaches zero, is zero. For a surface with an infinite number of asperities, distributed uniformly in space, it was shown in Ref. [5] that the static friction is zero as well. A modified version of this argument, which points out that for a surface with a finite number of asperities the static friction is nonzero, but smaller by a factor of a/L_0 compared to what it would be if the contributions of the asperities to static friction acted coherently, is provided in Appendix B of Ref. [6]. If this asperity is in the strong-pinning limit instead, we replace the factor of $c_a^{1/2}(L_0/a)$ by $c_a(L_0/a)^2$ to account for this, and as a result, the factor $c_a^{1/2}(L_0'/L_0)$ gets replaced by $c_a(L_0'/a)$, which could make the asperity satisfy the criterion for multistability more easily, and consequently, the friction from these asperities will no longer be reduced by the factor a/L_0. For a load per unit area, σ, assumed to be primarily due to hard-core interactions, we may assume $V_0\approx\sigma a^3/c$, where c is the fraction of the surface atoms which are in contact with the substrate. By the above arguments, $c=c_ac_0c_1c_2\cdots c_{n_m-1}$. Then, we see that the criterion for the zeroth-order asperity to be multistable is $\sigma>c_0c_1c_2\cdots c_{n_m-1}K$. If the criterion for weak pinning for the zeroth-order asperity surface is not satisfied, the criterion for monostability of this asperity gets changed from the above inequality to $(V_0/Ka^3)c_a(L_0'/a)<1$.

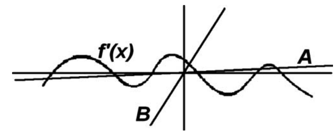

FIG. 3. This figure illustrates the solution of Eqs. (1)–(3), for Δx_0, Δx_1, and Δx_n, respectively. $f'(x)$ is a schematic illustration of the functions f_0', f_1', and f_n', and x denotes Δx_0, Δx_1, or Δx_n, respectively. Lines A and B represent the line $y=(Ka^3/V_0)(L_n/L_n')x$, for $(Ka^3/V_0)(L_n/L_n')<1$ and $(Ka^3/V_0)(L_n/L_n')>1$, respectively. For the situation illustrated by line A, there are multiple solutions (i.e., multistability), while for the situation illustrated by line B, there is only one (monostability).

At the next level, we have an asperity surface in contact with the substrate which consists of a collection of the lowest level (i.e., the smallest) asperities discussed in the previous paragraph. Assuming this asperity to be in the weak-pinning regime, the potential of interaction with the substrate, which is the sum of all of the interactions of the substrate with the lowest-order asperities, which cover a first-order asperity, is of order $V_0(c_ac_0)^{1/2}(L_0/a)(L_1/L_0)f_1(\Delta x_1/a)$. Here L_1 represents the width of this order asperity, Δx_1 represents a displacement of the lower surface of this level asperity for fixed (i.e., undistorted) configurations of all higher-order asperities, and f_1 denotes one of the functions which describe the interface potential energy of one of the first-order asperities. It has at least one minimum and runs over a range of magnitude 1 as its argument runs over a range of order 1. [The factor of $(c_ac_0)^{1/2}$ and c_ac_0, respectively, in these expressions were inadvertently not included in Ref. [6].] The elastic energy is of the order of $(1/2)L_1'L_1^2K(\Delta x_1/L_1')^2$, by the argument given above Eq. (1), where L_1' is the height of the body of the first-order asperity, which is assumed to be much larger than L_0'. Minimizing the sum of these two energies, we obtain

$$\Delta x_1/a \approx (V_0/Ka^3)(c_a c_0)^{1/2}(L_1'/L_1)f_1'(\Delta x_1/a). \quad (2)$$

Again, we conclude, based on the arguments presented in Ref. [5], that the static friction is reduced by a factor of L_0/L_1 below what it would be if the contributions to the static friction from each of the miniasperities at this level acted coherently. If the zeroth-order asperities attached to this first order asperity are in the strong-pinning regime, the factor of $(c_a c_0)^{1/2}L_1/L_0$ in the equation for the interaction of this asperity with the substrate is replaced by $c_a c_0(L_1/L_0)^2$, and hence, the right-hand side of Eq. (2) has the factor $(c_a c_0)^{1/2}L_1'/L_1$ replaced by $c_a c_0 L_1'/L_0$, which can make the solutions to this equation for Δx_1 multistable.

Continuing this procedure, we find that the displacement of the nth-level miniasperity is found by solving

$$\Delta x_n/a \approx (V_0/Ka^3)(c_a \cdots c_{n-1})^{1/2}(L_n'/L_n)f_n'(\Delta x_n/a), \quad (3)$$

where L_n and L_n' are the width and height of the body of the nth-level asperity. [The factor of $(c_a \cdots c_{n-1})^{1/2}$ in this expression was inadvertently not included in Ref. [6]. The general conclusions of Ref. [6], however, are not changed by this omission.] If $(V_0/Ka^3)(c_a \cdots c_{n-1})^{1/2} = \sigma/[K(c_n c_{n+1} \cdots c_{n_m})^{1/2}] > 1$ and $L_n'/L_n \sim 1$ for all n, asperities of all orders will be multistable, implying the occurrence of large static friction. If the condition given earlier for strong pinning at the zeroth-order asperity interface—namely, $\sigma > c_a^{1/2} c_0 c_1 \cdots c_{n_m} K = (c/c_a^{1/2})K$ is satisfied—the condition for multistability on all levels, $\sigma > (c_n c_{n+1} \cdots c_{n_m})^{1/2}K$, is certainly satisfied for the zeroth-order asperities, but may break down at some order n. Since more of the c's will appear in the product of the c's in this expression for lower-order than higher-order asperities, we conclude that the lower-order asperities are more likely to be multistable than the higher order ones. If the nth-order asperity is in the strong-pinning regime, the factor $(c_a \cdots c_{n-1})^{1/2}(L_n'/L_n)$ in Eq. (3) gets replaced by $(c_a \cdots c_{n-1})(L_n'/a)$, which leads to the condition for multistability: $\sigma > (c_n c_{n+1} \cdots c_{n_m})(L_n'/a)K$.

At least in the limit in which the stress acting on a given length-scale asperity resulting from the load that it carries is small compared to Young's modulus, recent theories of contact mechanics for surfaces with multi-length-scale roughness [9,10] show that the area of contact on all length scales (even the smallest) is approximately proportional to the applied load. This implies that although the smallest-length-scale asperities will certainly flatten out as the load increases (which means in the language of the present paper that a larger fraction of the subasperities on the surface of this asperity will come in contact with the second surface, and a similar picture holds for each of its subasperities). Consequently, on the basis of these theories, the amount of load carried by each of the atoms which are in contact with the second surface will not decrease as a consequence of more of these atoms being in contact with the second surface.

III. APPLICATION OF PERSSON'S CONTACT MECHANICS THEORY

Persson has developed an analytic contact mechanics theory for self-affine surfaces [10]. In Ref. [10], a differential equation is derived for the ratio of the contact area at the nth length scale to the nominal area of the interface A, i.e., $P(\zeta_n) = A(\zeta_n)/A$, as a function of the independent variable $\zeta_n = L/L_n$, known as the magnification. The picture provided in this theory is based on the following simple idea: If one imagines looking at the interface area with a hypothetical instrument of very poor resolution, one might not see the surface roughness on smaller length scales than $L = L_{n_m}$ (where L is the length or width of the interface). If one uses a hypothetical instrument of better resolution, one might see roughness on a length scale L_{n_m-1} (i.e., one might see asperities of size L_{n_m-1}), but roughness on smaller length scales (e.g., L_{n_m-2}) is not seen. In other words, on that length scale, the surface appears to be flat. With better resolution, one sees roughness on a length scale L_{n_m-3}, etc. The surface is assumed to be self-affine, meaning that the roughness seen on length scale L_n when all lengths parallel to the surface are multiplied by L_{n+1}/L_n, lengths perpendicular to the surface are multiplied by a factor $(L_{n+1}/L_n)^H$, where $0 < H < 1$. H is related to the fractal dimension D_f by $D_f = 3 - H$ [12,13]. The differential equation for $P(\zeta_n)$ is solved using the height-height correlation theory from the theory of roughness [12,13].

In Ref. [6], the roughness at the nth length scale was treated using the parameter c_n which denotes the fraction of nth-length-scale asperities which are in contact with the substrate, whereas Ref. [10] denotes the nth-length-scale roughness by the contact area at that length scale $A(\zeta_n)$, which is a potentially measurable quantity. Hence, there is much to be gained by expressing the results of Ref. [6] in terms of the parameters of Ref. [10]. Furthermore, by expressing the results of Ref. [6] in terms of the parameters of Ref. [10], it is possible to use the numerical estimates of the contact area found in Ref. [10] to estimate the conditions under which one is expected to have large or small friction. One important application of this approach is to obtain more accurate estimates of the conditions under which materials with large elastic constants and/or hardness might be able to function as good lubricants. Then, in this section, a connection will be made between the parameters used here and the contact area on a given length scale λ, $A(\zeta)$ used in Ref. [10], were $\zeta = L/\lambda$, where L is the largest length scale of the surface. On a length scale $\lambda = L_{n_m}$, there will be $(L_{n_m}/L_{n_m-1})^2$ asperities of lateral size L_{n_m-1}, a fraction c_{n_m-1} of which are in contact with the substrate. It is clear that L_{n_m} denotes the largest length scale, which represents the dimensions of the actual surface. On this surface, there will be $c_{n_m-2}(L_{n_m-1}/L_{n_m-2})^2$ contacting asperities of size L_{n_m-2}, and on each of these asperities, there will be $c_{n_m-3}(L_{n_m-2}/L_{n_m-3})^2$ contacting asperities of size L_{n_m-3}. As we continue, we reach the L_{n+1}-scale asperities, each of which contains $c_n(L_{n+1}/L_n)^2$ contacting asperities of linear dimension L_n. If we were to stop at this length scale and assume that the area of contact of each of these L_n-length-scale asperities is smooth (because we are imagining that our measuring instruments cannot see such small length scales), and the total area of contact of the surface with the substrate will be given by the product of the above numbers of contacting asperities at each length scale and L_n^2 (the cross-sectional area of an nth-scale asperity), or

$$P(\zeta_n) = A(\zeta_n)/A(\zeta_{n_m}) = c_{n_m-1}(L_{n_m}/L_{n_m-1})^2 c_{n_m-2}(L_{n_m-1}/L_{n_m-2})^2 c_{n_m-3}(L_{n_m-2}/L_{n_m-3})^2 \cdots c_n(L_{n+1}/L_n)^2\left(\frac{L_n^2}{A}\right) = c_{n_m-1}c_{n_m-2}c_{n_m-3}\cdots c_{n+1}c_n, \qquad (4)$$

where we have used the fact that $A(L_{n_m})=L_{n_m}^2$, and hence, the quantity $P(\zeta_n)=A(L_n)/A(L_{n_m})$ is a quantity used in Persson's theory [10], where the magnification $\zeta_n=L_{n_m}/L_n$. The largest length scale L_{n_m}, which will often be denoted by L, is the length of sliding solid, and $A=L^2$ is its nominal area. Using this relationship between Persson's $P(\zeta_n)$ and the quantity c_n used in Ref. [6] and, here, we can write the criterion for multistability of the nth-order asperity discussed under Eq. (3) of the last section as

$$\sigma > (a/L_n')P(\zeta_n)K = \frac{a}{L_n'}\frac{A(\zeta_n)}{A}K, \qquad (5)$$

assuming strong pinning at all asperity interfaces, and

$$\sigma > (L_n/L_n')[P(\zeta_n)P(\zeta_a)]^{1/2}K = \frac{L_n}{L_n'}\frac{[A(\zeta_n)A(\zeta_a)]^{1/2}}{A}K, \qquad (6)$$

where $\zeta_a=L_{n_m}/a$, assuming weak pinning. From Eqs. (5) and (6), it is clear that for sufficiently small $A(\zeta_n)$, the asperities will tend to be multistable, resulting in nonzero static and dry friction. By writing the criteria for multistability of the asperities in terms of Persson's $P(\zeta_n)$, we can use the results of his theory of contact mechanics to determine the load dependence of these criteria.

Let us now use the theory of Ref. [10] to determine the contact area per asperity at a particular length scale (call it the nth-length scale). Since the number of (n_m-1)-level asperities in contact is $c_{n_m-1}(L_{n_m}/L_{n_m-1})^2$ and the number of (n_m-2)-level asperities residing on one of the (n_m-1)-level asperities in contact is $c_{n_m-2}(L_{n_m-1}/L_{n_m-2})^2$, etc., we conclude that the number of nth-level asperities in contact is

$$c_{n_m-1}(L_{n_m}/L_{n_m-1})^2 c_{n_m-2}(L_{n_m-1}/L_{n_m-2})^2 \times c_{n_m-3}(L_{n_m-2}/L_{n_m-3})^2 \cdots c_n(L_{n+1}/L_n)^2, \qquad (7)$$

which is equal to

$$c_{n_m-1}c_{n_m-2}c_{n_m-3}\cdots c_n(L_{n_m}/L_n)^2 = A(L_n)/L_n^2. \qquad (8)$$

Using the fact that the contact area per nth-order asperity is equal to the nominal area of the interface $A(L_{n_m})$ divided by the above expression for the number of nth-level asperities in contact, we obtain for the mean contact area per asperity at the nth-level L_n^2, independent of the load. If we stop at nth-order in Persson's treatment [10], we take the surfaces at smaller length scales to be perfectly flat. In reality, there must also be a small enough length scale in Persson's theory in which asperities at all smaller length scales will get completely flattened out, if the solid is treated as being completely elastic, but of course long before that point, we must deal with plasticity. For the interested reader, the issue of asperity flattening is discussed in Appendix C for an earlier, although less complete, theory of multilength scale asperities due to Archard [14].

Persson shows using his theory of contact mechanics [10] the not unexpected result that as the magnification parameter $\zeta_n=L_{n_m}/L_n$ approaches infinity, $A_{el}(\zeta_n)/A$, where $A_{el}(\zeta_n)$ denotes the area of contact associated with elastic deformation of asperities, approaches zero. Then $E_YA_{pl}(\zeta_n)=\sigma A$, where $A_{pl}(\zeta_n)$ is the contact area associated with plastic deformation of asperities under load and E_Y denotes the hardness of the material (i.e., the compressional stress at which plastic deformation takes place). Some of Persson's arguments are summarized and some steps are filled in Appendix B. Generally, when the lowest-length-scale asperities have failed plastically under compression, if one attempts to shear the asperity by sliding the surfaces relative to each other, it will also have failed plastically in shear motion [15], and hence, either the resulting shear stress due to shearing of the asperity will be nearly independent of the shear strain or it will increase with shear strain, but much more slowly, as a function of shear strain, than it would if its response were elastic. In the latter case, the tendency towards multistability will be greatly increased over what it would be if the shear response were elastic, implying an increase in the dry and static friction. In the former case, the asperity would shear without any increased restoring force, most likely indicating that it will break as it shears relative to the substrate. This indicates that the system has switched over to a regime in which a good part of the kinetic friction is due to wear (i.e., the breaking of the smallest-length-scale asperities). The static friction will likely go to zero if this were a completely correct model for plastic flow, because in such a case, there is no energy cost to shear the asperity.

As mentioned earlier, Persson has demonstrated that as ζ_n approaches infinity, all parts of the contact area exhibit plasticity. (The argument is discussed in Appendix B of this article.) It is important, however, to estimate the value of ζ_n for which plastic deformation of asperities on the nth scale becomes important. The rough criterion that we will use to estimate this is when the mean value of the compressional stress over an nth-order asperity becomes comparable to the yield stress E_Y. One may determine when plasticity at the smaller-length-scale asperities sets in using Persson's theory, assuming that the distortions on all length scales are elastic until this point. Persson finds in the elastic regime the following expression for the contact area at nth-scale magnification:

$$\frac{A(\zeta_n)}{A} = P(\zeta_n) = \frac{4\sigma(1-\nu^2)}{q_0h_0E}\left(\frac{1-H}{\pi H}\right)^{1/2}\zeta_n^{(H-1)}, \qquad (9)$$

where $H=3-D_f$, where D_f is the fractal dimension of the surface, $q_0=2\pi/L$, h_0 is the rms surface height fluctuation, and ν is Poisson's ratio. Since we must have

$$\langle\sigma\rangle|_{\zeta_n} A(\zeta_n) = \sigma A, \tag{10}$$

$\langle\sigma\rangle|_{\zeta_n} = \sigma / P(\zeta_n)$, and hence, from Eq. (9), we have

$$\frac{\langle\sigma\rangle|_{\zeta_n}}{E} = \frac{q_0 h_0}{4(1-\nu^2)} \left(\frac{\pi H}{1-H}\right)^{1/2} \zeta_n^{(1-H)}. \tag{11}$$

When $\langle\sigma\rangle|_{\zeta_n}$ becomes comparable to E_Y, one must consider plasticity. Persson considers $H=0.8$, a value typical for pavement and q_0h_0 equal to 0.001 and 0.01. [Smaller values of H represent rougher surfaces, because by the definition of a self-affine surface, reducing the length scale along the surface by a factor λ (with $\lambda < 1$) reduces the height fluctuations only by a factor λ^H, and since $H<1$, larger height fluctuations occur over smaller lateral length scales.] Using these numbers in the above expression for $\langle\sigma\rangle|_{\zeta_n}$, we find that for $L/L_n = 10^8$, typical for atomic-level asperities, and $\langle\sigma\rangle|_{\zeta_n}/E \approx 0.04$ for $q_0h_0=0.001$ and 0.4 for $q_0h_0=0.01$. $E_Y/E=0.1$ for glass, 0.0013 for steel, and 0.0125 for hard plastic. Thus, atomic-scale asperities are clearly in the plastic regime. For diamond films, E_Y, the hardness, is about 100 GPa [16], and since E is 1080 GPa [17], $E_Y/E \approx 0.09$. Other diamondlike carbon films with large sp^3 (i.e., tetrahedral σ) bond content also exhibit E_Y/E of comparable magnitude. We see here the important role played by the relatively large values of E_Y/E that exist for these materials. On the basis of the above arguments, we conclude that it is possible for sufficiently smooth surfaces that for diamondlike carbon films, asperities on all length scales that exist for a crystalline material might be elastic.

At this point, let us reexamine the argument presented in Ref. [6], that the large values of Young's modulus of stiff coatings, such as diamondlike carbon films, can account for their excellent lubricating properties, making use of Eqs. (5), (6), and (9). Combining Eqs. (5) and (6) with Eq. (9), we obtain for the condition for the nth-order asperities to be multistable

$$\frac{K}{E} < \frac{L_n'}{a} \frac{q_0 h_0}{4(1-\nu^2)} \left(\frac{\pi H}{1-H}\right)^{1/2} \zeta_n^{(1-H)}, \tag{12a}$$

if the interfaces between each level asperity less than or equal to nth order are in the strong-pinning regime (defined in the previous two sections), or

$$\frac{K}{E} < \frac{L_n'}{L_n} \frac{q_0 h_0}{4(1-\nu^2)} \left(\frac{\pi H}{1-H}\right)^{1/2} (\zeta_n \zeta_a)^{(1-H)/2}, \tag{12b}$$

if the interfaces between each level asperity less than or equal to nth order are in the weak-pinning regime. Since the $n=0$ order asperities are the ones most likely to be multistable, let us apply Eqs. (12a) and (12b) to the $n=0$ case, for which they reduce to

$$\frac{K}{E} < \frac{L_0'}{a} \frac{q_0 h_0}{4(1-\nu^2)} \left(\frac{\pi H}{1-H}\right)^{1/2} \zeta_a^{(1-H)} \tag{13a}$$

and

$$\frac{K}{E} < \frac{L_0'}{L_0} \frac{q_0 h_0}{4(1-\nu^2)} \left(\frac{\pi H}{1-H}\right)^{1/2} \zeta_a^{(1-H)}, \tag{13b}$$

respectively. The condition for weak pinning at an $n=0$ asperity interface found in the last section is

$$\sigma < c_a^{1/2} (c_0 c_1 \cdots c_{n_m - 1}) K, \tag{14}$$

which when written in terms of Persson's notation [10] is

$$\sigma < c_a^{-1/2} \frac{A(\zeta_a)}{A} K. \tag{15}$$

Substituting for $A(\zeta_a)/A$ using Eq. (9), this condition can be written as

$$\frac{K}{E} > \frac{c_a^{1/2} q_0 h_0}{4(1-\nu^2)} \left(\frac{\pi H}{1-H}\right)^{1/2} \zeta_a^{(1-H)}. \tag{16}$$

As can be seen from Eqs. (13b) and (16), in order for the zeroth-order asperities to be multistable and at the same time have their interfaces with the substrate in the weak-pinning limit, we must have $c_a^{1/2} < L_0'/L_0$, which is not difficult to satisfy unless the zeroth-order asperities are all extremely short and thick and/or have a large fraction of the atoms at their interfaces in contact with the second surface.

IV. CONCLUSIONS

It has been shown, using a scaling theory of friction for surfaces with multiscale roughness [6] combined with Persson's theory of contact mechanics that, in contrast to surfaces with only single-scale roughness which appear to always exhibit superlubricity, unless one postulates the existence of mobile dirt particles at the interface, clean surfaces with multiscale roughness will almost always exhibit static and dry friction, characteristic of almost all solid surfaces. The static and dry friction come about because asperities at the smallest length scales will be multistable, because they support all of the load if they remain elastic or will exhibit plastic failure. Combining the scaling theory of Ref. [6] with the analytic contact mechanics theory of Ref. [10] allows us to relate the occurrence of static and dry friction (i.e., kinetic friction in the slow sliding speed limit) to the contact area at various length scales. It also allows us to determine the conditions under plastic deformation is expected to be important, and a discussion was given of how plastic deformation affects the occurrence of static and dry friction. By combining the results of Refs. [6,10], it was possible to make more precise statements than was possible using the methods of Ref. [6] alone concerning the conditions under which surfaces coated with materials with high shear elastic constants will lead to low friction, by expressing the criterion for this to occur in terms of parameters describing the nature of the roughness of the surface, in addition to the elastic constants. Numerical finite-element calculations used recently to study contact mechanics [9] can also be applied to this problem. Since they appear to yield results for the contact mechanics problem which are qualitatively similar to those of Ref. [10], however, the results for the multistability (i.e., Tomlinson model [5]) problem should not differ significantly from those presented here. There is one small difference, however, which is worth considering. Whereas Ref. [10] finds that $A(\zeta_n)/A$ is a linear function of σ in the elastic regime, Ref. [9] reports that this function is a slightly sublinear function of σ. As already suggested in Ref. [6], this would imply that as σ increases, the interface could possibly switch from having all asperities in the monostable regime, resulting in low friction, to the multistable regime, resulting in high friction, when σ becomes sufficiently large.

The issue has been raised in the literature [18] that thermal energy could under the right circumstances eliminate Tomlinson-model instabilities. In the context of the model studied in this article, in which for macroscopic surfaces there will be an infinite number of lowest-length-scale asperities in contact with the second surface, such thermal activation effects will likely lead to creep motion in which the two surfaces when under shear stress, even below the force of static friction, will slide over very long time scales. In future work the question of whether the present model can account for the observed magnitudes of such creep motion will be explored.

APPENDIX A: EFFECTS OF ASPERITY SHAPE ON FRICTION

In Sec. III, we assumed that the actual shape of an asperity would have an insignificant effect on the multiscale Tomlinson model that has been developed here. In this section, we will examine whether this is likely to be a reasonable assumption. Asperities on all length scales are likely to initially be peaked, but as they are pressed together, they flatten out. The amount of flattening of a given length scale asperity depends on the amount of load that asperity carries, which itself depends on the degree of compression of the asperity, as is known to happen for single-length-scale asperities [11]. The amount of load carried by an asperity depends on the number of atoms in contact with the substrate, as we have seen earlier that each atom carries a load of the order of Pa^2/c. Typically, near the peak of an asperity at any length scale, the profile can be represented to a good approximation by a paraboloid whose cross-sectional area at a distance z from apex is proportional to z [11]. It is not a bad approximation to assume that we can use this result for an asperity which gets compressed because it is in contact with the substrate. Then let us assume that a compressed asperity has a flat peak at a minimum value of z (z_{min}), whose area is proportional to z_{min}. Then, using the paraboloid approximation for the asperity, we have $\pi r^2 \approx 2\pi Rz$, let us imagine slicing each such asperity into slices of thickness Δz, each of whose area is proportional to z. Then, the shear stress between slices n and $n+1$ is equal to

$$(2\pi R z_n/a)K\left[\left(\frac{u_{n+1}-u_n}{a}\right)z_{n+1}-\left(\frac{u_n-u_{n-1}}{a}\right)z_n\right], \quad \text{(A1)}$$

following the method for taking the continuum limit of the harmonic approximation treatment of a discrete lattice discussed in Ref. [19]. This must be zero when the asperity is in equilibrium. The continuum limit of this equation is

$$\frac{\partial}{\partial z}\left(\frac{\partial(zu)}{\partial z}\right)=0, \quad \text{(A2)}$$

whose solution is

$$\frac{\partial u}{\partial z}=\frac{c}{z}, \quad \text{(A3)}$$

where c is a constant. Since at $z=z_{min}$, we require that $K(\pi r_c^2)(\partial u/\partial z)|_{z=z_{min}}=\sigma\pi r_c^2$, where r_c is the contact radius and σ is the shear stress acting on the contact area of the asperity, because this is the condition for equilibrium of the asperity. This gives us $c=\sigma z_{min}/K$. Then, $\partial u/\partial z=(\sigma z_{min}/Kz)$. We may find the elastic energy of an asperity from

$$E_{elast}=(1/2)\int_{z_{min}}^{z_{max}} dz\, 2\pi RzK\left(\frac{\partial u}{\partial z}\right)^2$$
$$=[\pi R(\sigma z_{min})^2/K]\int_{z_{min}}^{z_{max}}\frac{dz}{z}=[\pi R(\sigma z_{min})^2/K]\ln\left(\frac{z_{max}}{z_{min}}\right). \quad \text{(A4)}$$

In order to compare this with the expression used in the scaling treatment of multiscale asperities used in Ref. [6] and here, let us now write this expression in terms of Δu, given by

$$\Delta u=(\sigma z_{min}/K)\int_{z_{min}}^{z_{max}}\frac{dz}{z}=(\sigma z_{min}/K)\ln\left(\frac{z_{max}}{z_{min}}\right). \quad \text{(A5)}$$

Solving for σ in terms of Δu and substituting in the above expression for E_{elast}, we obtain

$$E_{elast}=\frac{\pi KR}{\ln\left(\frac{z_{max}}{z_{min}}\right)}\Delta u^2=\frac{K\pi L^2 z_{max}}{2\ln\left(\frac{z_{max}}{z_{min}}\right)}\left(\frac{\Delta u}{z_{max}}\right)^2, \quad \text{(A6)}$$

where L is defined by $\pi L^2=\pi r_{max}^2=2\pi R z_{max}$. For the nth-order asperity, we identify L with L_n and $z_{max}-z_{min}$ with L_n'. Since for all except for the extremes of complete compression and nonexistent compression z_{max} and $z_{max}-z_{min}$ are of comparable magnitudes and $\ln(z_{max}/z_{min})$ contributes only a factor of order unity, we conclude that our original scaling treatment of multiscale asperity multistability, which does not consider the actual shape of the asperities, will give the correct orders of magnitude.

APPENDIX B: DEMONSTRATION OF THE OCCURRENCE OF COMPLETELY PLASTIC CONTACT AT VERY SMALL LENGTH SCALES

In Appendix C of Persson's paper on contact mechanics [10], he obtains a differential equation for the area of contact due to plastic deformation alone by integrating his diffusion equation,

$$\frac{\partial P(\sigma,\zeta)}{\partial \zeta}=f(\zeta)\frac{\partial^2 P(\sigma,\zeta)}{\partial \sigma^2}, \quad \text{(B1)}$$

over σ, to obtain

$$\frac{\partial}{\partial \zeta}\int_0^{\sigma_Y} d\sigma\, P(\sigma,\zeta) = f(\zeta)\left(-\left.\frac{\partial P(\sigma,\zeta)}{\partial \sigma}\right|_{\sigma=0} + \left.\frac{\partial P(\sigma,\zeta)}{\partial \sigma}\right|_{\sigma=\sigma_Y}\right). \quad \text{(B2)}$$

The integral $\int_0^{\sigma_Y} d\sigma\, P(\sigma,\zeta)$ is by definition $P(\zeta)=A_{el}(\zeta)/A$. The first term on the right-hand side of Eq. (B2) was shown in Ref. [10] to be equal to $-dA_{non}(\zeta)/d\zeta$, the negative of the derivative of the surface area not in contact with respect to ζ. In the limit as σ_Y approaches infinity, the second term on the right-hand side of Eq. (B2) vanishes. Since in this limit there is clearly only elastic deformation, the latter term must be associated with plastic deformation. Then in this limit, Eq. (B2) can be written as

$$\frac{dA_{el}}{d\zeta} + \frac{dA_{non}}{d\zeta} = 0, \quad \text{(B3)}$$

and hence $A_{el}+A_{non}$ must equal a constant A in this limit and that constant must be A. Then, clearly when σ_Y is finite, we must identify the last term on the right-hand side of Eq. (B2) with $dA_{pl}/d\zeta$. Using his solution for $P(\sigma,\zeta)$ Persson finds by integrating this expression that

$$P_{pl}(\zeta) = \frac{A_{pl}(\zeta)}{A} = -(2/\pi)\sum_{n=1}^{\infty}(-1)^n \frac{\sin\alpha_n}{n} \times\left[1-\exp\left(-\alpha_n^2\int_1^{\zeta} d\zeta' g(\zeta')\right)\right], \quad \text{(B4)}$$

where $\alpha_n = n\pi\sigma_0/\sigma_Y$, and

$$P_{non}(\zeta) = \frac{A_{pl}(\zeta)}{A} = (2/\pi)\sum_{n=1}^{\infty}\left(\frac{\sin\alpha_n}{n}\right)[1-\exp(-\alpha_n^2)],$$

$$P_{pl}(\zeta) = \frac{A_{pl}(\zeta)}{A} = -(2/\pi)\sum_{n=1}^{\infty}(-1)^n\left(\frac{\sin\alpha_n}{n}\right) \times\left[1-\exp\left(-\alpha_n^2\int_1^{\zeta} d\zeta' g(\zeta')\right)\right]. \quad \text{(B5)}$$

Since as ζ approaches infinity $\int_1^{\zeta} d\zeta' g(\zeta')$ approaches infinity, we find that in the infinite ζ limit, the sum of Eqs. (B4) and (B5) becomes

$$P_{non} + P_{pl} = \frac{A_{non}(\zeta)}{A} + \frac{A_{pl}(\zeta)}{A} = \frac{4}{\pi}\sum_{n=1,odd}^{\infty}\frac{\sin\left(\frac{n\pi\sigma_0}{\sigma_Y}\right)}{n} = 1 \quad \text{(B6)}$$

by a well-known identity, which implies that none of the asperities at the regions of contact for $\zeta=\infty$ are in elastic contact. Since there is no stress acting on the area A_{non} by definition and $\sigma=\sigma_Y$ at all areas of plastic contact, we must have

$$\sigma_Y A_{pl} = \sigma A. \quad \text{(B7)}$$

This result also follows if we take the ζ approaches infinity limit in Eq. (B4), making use of the identity

$$-x = \frac{2}{\pi}\sum_n (-1)^n \sin(n\pi x) \quad \text{(B8)}$$

for $-1 < x < 1$.

APPENDIX C: A DEMONSTRATION THAT ARCHARD'S MODEL OF MULTISCALE ASPERITIES PREDICTS THAT THE CONTACT AREA PER ASPERITY INCREASES WITH INCREASING LOAD

It is interesting to note that if we calculate the area per nth-order asperity using Archard's theory of contact mechanics for fractal surfaces [14], we find that it is proportional to the load to a power which decreases as n decreases, implying that even if the surface is assumed to be perfectly elastic, the smaller-length-scale asperities will flatten out at sufficiently high load, provided that we put a small-length-scale cutoff in his theory.

In Archard's model [14] for elastic distortion of multiscale asperities at the longest length scale an asperity has a hemispheric shape and distorts according to Hertz theory [11]. The area of contact of such an asperity with a flat surface is assumed to be covered by a continuous distribution of smaller-scale hemispherically shaped asperities. The largest-length-scale asperity described above is only in contact at the areas of contact of these smaller asperities. The smaller asperities are in turn also assumed to be in contact only at the locations of a continuous distribution of still smaller asperities. Archard argues that as we consider shorter and shorter length scales, the contact area becomes more and more nearly proportional to the load carried by the original longest-length-scale asperity.

At his longest length scale, Archard finds that the contact area is proportional to $W^{2/3}$, where W is the load and the asperity density is independent of load. At the next smaller length scale considered by him, the contact area is proportional to $W^{8/9}$ and the number density of these asperities is proportional to $W^{2/3}$, and hence the contact area per asperity (i.e., the quotient of these two) is proportional to $W^{2/9}$. At the next smaller length scale, the contact area is proportional to $W^{26/27}$ and the asperity density is proportional to $W^{8/9}$, leading to a contact area per asperity (the quotient of the contact area and asperity density) of $W^{2/27}$. Next order gives a contact area proportional to $W^{44/45}$ with an asperity distribution proportional to $W^{26/27}$, leading to a contact area per asperity of $W^{2/135}$. As we continue this process, the asperity density is always proportional to the same power of W as the contact area at the previous length scale. Hence, it is clear that as we go to successively smaller length scales, the contact area per asperity is proportional to a smaller and smaller power of W. Thus, it is clear that as W increases, the smaller-length-scale asperities' contact area will grow, suggesting that the smallest-length-scale asperities will flatten out as the load increases, since the amount that asperities on smaller and smaller length scales flatten out as a function of W decreases as we go to smaller and smaller length scales. Since this theory does not assign a precise radius to each length scale asperity, it is difficult to assess the degree to which smaller-length-scale asperities flatten out (i.e., how the contact area per asperity compares to the original size of an asperity). Since the contact area at each length scale appears to be proportional to the inverse asperity density raised to the same power as the power of W that the contact area is proportional to at that length scale, we can take that quantity as related to the original asperity size. Since the contact area per asperity grows as W to a smaller power, it is possible that the asperities do not flatten out in Archard's model, in the sense that the contact area remains small compared to the asperity size as W increases.

[1] M. H. Muser, in *Dynamics of Small Confing Systems V*, edited by J. M. Drake, J. Klefter, P. Levitz, R. M. Overney, and M. Urbakh, MRS Symposium Proceedings No. 651 (Materials Research Society, Warrendale, Pa, 2001); G. He, M. H. Muser, and M. O. Robbins, Science **284**, 1650 (1999); M. H. Muser and M. O. Robbins, Phys. Rev. B **61**, 2335 (2000); M. H. Muser, L. Wenning, and M. O. Robbins, Phys. Rev. Lett. **86**, 1295 (2001); G. He and M. Robbins, Tribol. Lett. **10**, 7 (2001); M. H. Muser, Phys. Rev. Lett. **89**, 224301 (2002).

[2] M. Hirano and K. Shinjo, Phys. Rev. B **41**, 11837 (1990); K. Shinjo and M. Hirano, Surf. Sci. **283**, 473 (1993); S. Aubry, in *Solitons and Condensed Matter*, edited by A. R. Bishop and T. Schneider (Springer, Berlin, 1978), p. 264; J. E. Sacco and J. B. Sokoloff, Phys. Rev. B **18**, 6549 (1978); M. Hirano, in *Superlubricity*, edited by A. Erdimir and J. M. Martin (Elsevir, Boston, 2007), pp. 17–38; J.-M. Martin, C. Donnet, and T. Le Mogne, Phys. Rev. B **48**, 10583 (1993); J.-M. Martin, C. Donnet, T. Le Mogne, and J. L. Loubert, Surf. Coat. Technol. **68/69**, 427 (1994); C. Grossiord, K. Valot, J.-M. Martin, T. Le Mogne, C. Esnouf, and K. Inoue, Tribol. Int. **31**, 737 (1998); C. Grossiord, J.-M. Martin, T. Le Mogne, and K. Inoue, J. Vac. Sci. Technol. A **17**, 884 (1990); J.-M. Martin, in *Superlubricity*, edited by A. Erdimir and J. M. Martin (Elsevier, Boston, 2007), pp. 207–226.

[3] A. Volmer and T. Natterman, Z. Phys. B: Condens. Matter **104**, 363 (1997); J. B. Sokoloff, Phys. Rev. Lett. **86**, 3312 (2001); Phys. Rev. B **65**, 115415 (2002).

[4] J. B. Sokoloff, Phys. Rev. E **71**, 056107 (2005).

[5] C. Caroli and Ph. Nozieres, Eur. Phys. J. B **4**, 233 (1998); *Physics of Sliding Friction*, edited by B. N. J. Persson and E. Tosatti, Vol. 311 of *NATO Advanced Study Institute, Series E: Applied Sciences* (Kluwer Academic, Dordrecht, 1996); M. Brillouin, *Notice sur les Travaux Scientifiques* (Gautier-Villars, Paris 1909); G. A. Tomlinson, Philos. Mag. **7**, 905 (1929).

[6] J. B. Sokoloff, Phys. Rev. E **73**, 016104 (2006).

[7] C. Campana, Phys. Rev. B **75**, 155419 (2007).

[8] J. A. Heimberg, K. J. Wahl, and I. L. Singer, Appl. Phys. Lett. **78**, 2449 (2001); G. T. Gao, P. T. Mikulski, and J. A. Harrison, J. Am. Chem. Soc. **124**, 7202 (2002); G. T. Gao, P. T. Mikulski, G. M. Chateauneuf, and J. A. Harrison, J. Phys. Chem. B **107**, 11082 (2003); J. A. Harrison, C. T. White, R. J. Colton, and D. W. Brenner, Phys. Rev. B **46**, 9700 (1992); S. Dag and S. Ciraci, *ibid.* **70**, 241401(R) (2004); Y. Qi, E. Konca, and A. T. Alpas, Surf. Sci. **600**, 2955 (2006).

[9] S. Hyun, L. Pei, J. F. Molinari, and M. O. Robbins, Phys. Rev. E **70**, 026117 (2004); M. O. Robbins (unpublished).

[10] B. N. J. Persson, J. Chem. Phys. **115**, 3840 (2001); Phys. Rev. Lett. **87**, 116101 (2001).

[11] K. L. Johnson, *Contact Mechanics* (Pergamon Press, New York, 1985), pp. 90–95.

[12] J. Feder, *Fractals* (Plenum, New York, 1988).

[13] E. Bouchaud, J. Phys.: Condens. Matter **9**, 4319 (1997).

[14] J. F. Archard, Proc. R. Soc. London, Ser. A **243**, 190 (1957).

[15] G. C. Spencer, *Introduction to Plasticity* (Chapman and Hall, London 1968).

[16] P. Lemoine, J. P. Quinn, P. D. Maguire, and J. A. McLaughlin, *Tribology of Diamond-Like Carbon Films: Fundamentals and Applications* (Springer, Berlin, 2007).

[17] C. Kittel, *Introduction to Solid State Physics* (Wiley, New York, 1956), p. 93.

[18] L. Prandtl, Z. Angew. Math. Mech. **8**, 85 (1928); S. Yu. Krylov, K. B. Jinesh, H. Valk, M. Dienwiebel, and J. W. M. Frenken, Phys. Rev. E **71**, 065101(R) (2005). There are many other recent references that discuss this issue in the context of AFM experiments in the latter reference.

[19] N. W. Ashcroft and N. D. Mermin, *Solid State Physics* (Holt Rinehart and Winston, Philadelphia, 1976), pp. 443–447.